

identified,⁷¹ the present study is the first demonstration of this phenomenon for platinated duplex DNA. This assignment was made by means of a careful analysis of platinum stereochemistry with the aid of ¹⁵N NMR spectroscopy. In addition, modification of the amine ligands in the platinum coordination sphere has been shown to influence the selectivity for d(ApG) and d(GNG) intrastrand cross-link formation. The observed reduction in the number of d(ApG) cross-links suggests the exciting possibility that the mutagenic activity of compounds **1** and **2** may be decreased relative to cisplatin. The selective formation of the two d(GpG)-2 orientational isomers, corresponding to the 3' versus 5' orientation of the cyclohexylamine ligand, has been shown to play a small but measurable role in the processing of DNA platinated with complex **2**. In particular, both isomers are slightly less efficient than cisplatin in blocking replication despite the increased bulk of the platinum lesion, and each terminates DNA synthesis to different degrees at the two observed sites. The availability of high-resolution X-ray structural studies of cisplatin and related

complexes bound to duplex DNA will help in the understanding of the hydrogen bonding or steric factors that are responsible for these differences and should provide a basis for analyzing the relationship between the structures of specific platinum-DNA adducts and their processing by cellular components. Studies toward this end are in progress, from which may ultimately arise a rational basis for platinum antitumor drug design.

Acknowledgment. This work was supported by a grant from the National Cancer Institute of the National Institutes of Health (CA 34992). J.F.H. thanks the American Cancer Society for a postdoctoral fellowship. We are grateful to Drs. C. M. Giandomenico and M. J. Abrams at Johnson Matthey Biomedical Research for preprints and cisplatin, to the Stable Isotopes Laboratory at Los Alamos National Laboratory for providing ¹⁵N-2'-deoxyguanosine, to Dr. C. E. Costello at MIT for FAB-(MS/MS) spectra, and to Dr. K. M. Comess for helpful discussions.

Supplementary Material Available: Figure S1, displaying the FAB (MS/MS) spectrum of the d(ApG)-2 adduct (1 page). Ordering information is given on any current masthead page.

(71) Alink, M.; Nakahara, H.; Hirano, T.; Inagaki, K.; Nakanishi, M.; Kidani, Y.; Reedijk, J. *Inorg. Chem.* 1991, 30, 1236.

Dihydrogen Complexes of Metalloporphyrins: Characterization and Catalytic Hydrogen Oxidation Activity

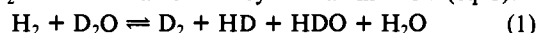
James P. Collman,^{*,†} Paul S. Wagenknecht,[†] James E. Hutchison,[†] Nathan S. Lewis,^{†,‡} Michel Angel Lopez,[†] Roger Guilard,^{†,§} Maurice L'Her,^{†,||} Aksel A. Bothner-By,[⊥] and P. K. Mishra[⊥]

Contribution from the Departments of Chemistry, Stanford University, Stanford, California 94305, and Carnegie Mellon University, Pittsburgh, Pennsylvania 15213. Received October 21, 1991

Abstract: A series of monometallic dihydrogen complexes of the type M(OEP)(L)(H₂) (M = Ru, Os; L = THF, *Im) was synthesized and characterized by ¹H NMR. The H-H bond length was found to increase when Os was replaced by Ru or when *Im was replaced by THF. The bond distances (as determined by T₁) range from 0.92 to 1.18 Å. The first example of a bimetallic bridging dihydrogen complex, Ru₂(DPB)(*Im)₂(H₂), was also prepared. The H₂ ligand is simultaneously bound to both Ru-metal centers. High-field ¹H NMR experiments (620 MHz) revealed a -7.37 Hz dipolar splitting of the H₂ ligand for this complex. Analysis of this splitting suggests that the H₂ ligand is bound with the H-H axis perpendicular to the Ru-Ru axis. These complexes were examined as possible catalysts for the oxidation of dihydrogen through prior heterolytic activation of H₂. Only Ru(OEP)(THF)(H₂) can be conveniently deprotonated. Ru(OEP)(THF)(H₂) is also implicated in the Ru(OEP)(THF)₂ catalyzed isotopic exchange between H₂ and D₂O in THF solution. Each step for this mechanism has been elucidated. We have also achieved catalytic dihydrogen oxidation using [Ru(OEP)]₂ adsorbed onto graphite. Two mechanisms for this ruthenium porphyrin catalyzed dihydrogen oxidation are presented and compared.

Though thermodynamically unstable in an oxygen atmosphere, dihydrogen is kinetically inert and is not reactive unless activated with a suitable catalyst. Such catalysis occurs naturally in certain microorganisms that have been known since the turn of the century to consume dihydrogen.¹ In 1931, Stephenson and Strickland² proposed the first description of this phenomenon in terms of enzymatic activation of hydrogen and named the relevant enzymes hydrogenases. The physiological role of hydrogenases is to mediate the production and consumption of dihydrogen in the presence of cofactors such as nicotinamide adenine dinucleotide, cytochrome c₃, and ferredoxin.^{3,4} However, an important criterion for hyd-

rogenase activity is the physiologically unimportant exchange of H₂ and D₂O first characterized by Farkas in 1934 (eq 1).^{5,6}



Several authors^{3,7} have suggested that this activity indicates

(1) (a) Pakes, W. C. C.; Jollyman, W. H. *J. Chem. Soc.* 1901, 79, 386-391. (b) Harden, A. *J. Chem. Soc.* 1901, 79, 601-628.

(2) Stephenson, M.; Strickland, L. H. *Biochem. J.* 1931, 25, 205-214.

(3) Holm, R. H. In *Biological Aspects of Inorganic Chemistry*; Addison, A. W., Cullen, W. R., Dolphin, D., James, B. R., Eds.; Wiley: New York, 1977; pp 71-112.

(4) Schlegel, H. G.; Schneider, K. In *Hydrogenases: Their Catalytic Activity, Structure and Function*; Schlegel, H. G., Schneider, K., Eds.; Verlag-Erich Goltze KG: Göttingen, 1978; pp 15-44.

(5) Farkas, A.; Farkas, L.; Yudkin, J. *Proc. R. Soc. London A* 1934, B115, 373.

(6) Several authors have now reported this exchange. (a) Lespinat, P. A.; Berlier, Y.; Fauque, G.; Czechowski, M.; Dimon, B.; LeGall, J. *Biochimie* 1986, 68, 55-61. (b) Arp, D. J.; Burris, R. H. *Biochim. Biophys. Acta* 1982, 700, 7-15. (c) Teixeira, M.; Fauque, G.; Moura, I.; Lespinat, P. A.; Berlier, Y.; Prickril, B.; Peck, H. D., Jr.; Xavier, A. V.; LeGall, J.; Moura, J. J. G. *Eur. J. Biochem.* 1987, 167, 47-58 and references therein.

[†] Stanford University.

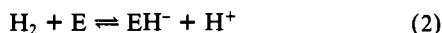
[‡] Present address: Division of Chemistry and Chemical Engineering, California Institute of Technology, Pasadena, CA 91125.

[§] Present address: Université de Bourgogne, Laboratoire de Synthèse et d'Electrosynthèse Organométallique Associé au CNRS (UA 33), Faculté des Sciences "Gabriel", 21100 Dijon Cedex, France.

^{||} Present address: U.R.A. C.N.R.S. 322, Faculté des Sciences, Université de Bretagne Occidentale, 6 Avenue V. Le Gorgeu, 29287 Brest Cedex, France.

[⊥] Carnegie Mellon University.

heterolytic activation of dihydrogen. In fact, in 1954 Krasna and Rittenberg⁷ first proposed that many of the functions of hydrogenase enzymes proceed through heterolytic activation of dihydrogen to form an active hydride (eq 2). The isotopic exchange



between H₂ and D₂O is then explained in terms of heterolytic hydrogen activation, followed by proton exchange. Functional hydrogenase enzyme models which catalyze the isotopic exchange process in eq 1 and which catalyze substrate reduction using dihydrogen have been published by Halpern⁸ and Henrici-Olivé.⁹

The recent discovery of dihydrogen complexes has sparked interest in their possible intermediacy in dihydrogen activation.¹⁰ The high acidities of some metal bound dihydrogen ligands¹¹ imply their possible intermediacy in the heterolytic activation of dihydrogen. Such reactivity led Crabtree to propose the intermediacy of metal bound dihydrogen and hydrides in hydrogenase enzyme reactivity.¹² More recently Albeniz et al.¹³ reported several dihydrogen complexes which catalyze the exchange given in eq 1. Additionally, Zimmer et al.¹⁴ reported a Ni-S complex, which more closely resembles the structure of hydrogenase enzymes, that also catalyzes this exchange.

We previously reported^{15,16} that metalloporphyrin hydrides and dihydrogen complexes can perform many of the same functions as hydrogenase enzymes: H₂/D₂O exchange, dihydrogen activation, and nicotinamide reduction. Because the mechanisms of this reactivity are more easily studied with these discreet metalloporphyrins than with large protein enzymes, we sought to extend our study of metalloporphyrin dihydrogen complexes presuming that their reactions may give insight into hydrogenase reactivity.

Herein, we describe the preparation of several new dihydrogen complexes of metalloporphyrins, including the first example of a complex in which dihydrogen bridges two metal centers. Data from our previously characterized dihydrogen complexes^{15,17} are included here for completeness and comparison. The reactivity of these dihydrogen complexes is examined, with special attention given to the deprotonation of the dihydrogen ligand as a possible means of dihydrogen activation. We have also demonstrated catalytic dihydrogen oxidation, near the thermodynamic potential, with an electrode treated with a metalloporphyrin. Evidence is presented for the intermediacy of a dihydrogen complex in this process as well as in the metalloporphyrin catalyzed exchange between H₂ and D₂O.

Results

Synthesis of the Dihydrogen Complexes M(OEP)(L)(H₂). The monomeric dihydrogen complexes Ru(OEP)(THF)(H₂) and Os(OEP)(*Im)(H₂)¹⁸ were prepared by protonation of the corresponding metalloporphyrin hydride anions¹⁶ K[M(OEP)(L)(H)]

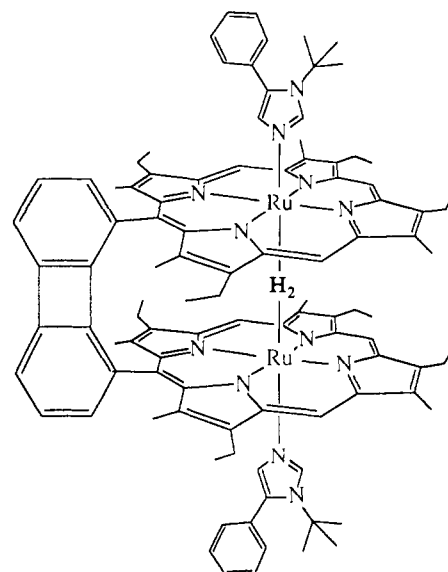
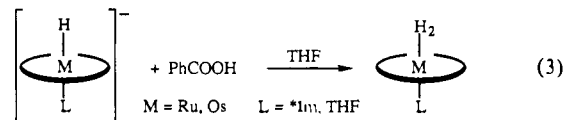
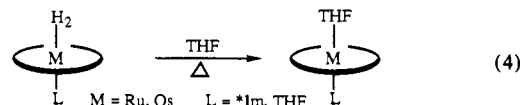


Figure 1. Proposed structure of Ru₂(DPB)(*Im)₂(H₂).

(M = Ru, Os; L = *Im, THF) with benzoic acid at -78 °C in THF-*d*₈ solvent (eq 3). Decomposition of the resulting H₂

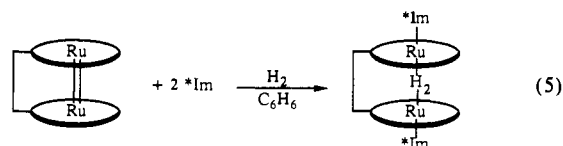


complexes was followed by ¹H NMR while raising the temperature and collecting a spectrum every 10 °C. Upon warming, the dihydrogen complexes decompose by replacement of H₂ with THF to form the corresponding M(OEP)(L)(THF) (eq 4). Significant



decomposition of the dihydrogen complexes Os(OEP)(*Im)(H₂) and Ru(OEP)(THF)(H₂) occurred at -20 and -30 °C, respectively. Attempts to synthesize Ru(OEP)(*Im)(H₂) by protonation of the K[Ru(OEP)(*Im)(H)] with benzoic acid in THF-*d*₈ were unsuccessful. The product from this reaction was Ru(OEP)(*Im)(THF),¹⁶ consistent with protonation of the metal hydride followed by rapid loss of dihydrogen. Similar attempts in toluene-*d*₈ resulted in no bound dihydrogen. Os(OEP)(THF)(H₂) was synthesized by protonation of the K[Os(OEP)(THF)(H)] in THF-*d*₈ at room temperature.¹⁵ This complex decomposes over the course of 1 day to form Os(OEP)(THF)₂. In THF-*d*₈, the THF ligand on all of the above complexes is not observed in the ¹H NMR spectrum due to exchange with THF-*d*₈. However, Os(OEP)(THF)(H₂) has also been synthesized by protonation of K[Os(OEP)(THF)(H)] in toluene-*d*₈ at -78 °C; in this case the trans THF ligand was detected by ¹H NMR spectroscopy. All of the dihydrogen complexes display sharp diamagnetic ¹H NMR resonances, with the methylene protons of the OEP ethyl substituents appearing as a multiplet, indicating that the two faces of the porphyrin are inequivalent. This precludes the assignment of these resonances to trans dihydrides.

Synthesis of the Bridged Dihydrogen Complex. Addition of 2 equiv of 1-*tert*-butyl-5-phenylimidazole (*Im) to a hydrogen-saturated benzene solution of the cofacial metalloporphyrin dimer, Ru₂(DPB), results in the immediate formation of Ru₂(DPB)(*Im)₂(H₂) (eq 5 and Figure 1). The ¹H NMR data supporting



(7) Krasna, A. I.; Rittenberg, D. *J. Am. Chem. Soc.* **1954**, *76*, 3015–3020.

(8) (a) Halpern, J.; James, B. *Can. J. Chem.* **1966**, *44*, 671–675. (b) Harrod, J. F.; Ciccone, S.; Halpern, J. *Can. J. Chem.* **1961**, *39*, 1372–1376.

(9) Henrici-Olivé, G.; Olivé, S. *J. Mol. Catal.* **1976**, *1*, 121–135.

(10) Kubas, G. *J. Acc. Chem. Res.* **1988**, *21*, 120–128.

(11) (a) Chinn, M. S.; Heinekey, D. M.; Payne, N. G.; Sofield, C. D. *Organometallics* **1989**, *8*, 1824–1826. (b) Jia, G.; Morris, R. H. *Inorg. Chem.* **1990**, *29*, 581–582. (c) Jia, G.; Morris, R. H.; Schweitzer, C. T. *Inorg. Chem.* **1991**, *30*, 593–594. (d) Jia, G.; Morris, R. H. *J. Am. Chem. Soc.* **1991**, *113*, 875–883. (e) Crabtree, R. H.; Lavin, M.; Bonneviot, L. *J. Am. Chem. Soc.* **1986**, *108*, 4032–4037. (f) Chinn, M. S.; Heinekey, D. M. *J. Am. Chem. Soc.* **1987**, *109*, 5865–5867. (g) Chinn, M. S.; Heinekey, D. M. *J. Am. Chem. Soc.* **1990**, *112*, 5166–5175.

(12) Crabtree, R. H. *Inorg. Chim. Acta* **1986**, *125*, L7–L8.

(13) Albeniz, A. C.; Heinekey, D. M.; Crabtree, R. H. *Inorg. Chem.* **1991**, *30*, 3632–3635.

(14) Zimmer, M.; Schulte, G.; Luo, X.-L.; Crabtree, R. H. *Angew. Chem., Int. Ed. Engl.* **1991**, *30*, 193–194.

(15) Collman, J. P.; Wagenknecht, P. S.; Hembre, R. T.; Lewis, N. S. *J. Am. Chem. Soc.* **1990**, *112*, 1294–1295.

(16) Following paper in this issue.

(17) Collman, J. P.; Hutchison, J. E.; Wagenknecht, P. S.; Lopez, M. A.; Guillard, R.; Lewis, N. S. *J. Am. Chem. Soc.* **1990**, *112*, 8206–8207.

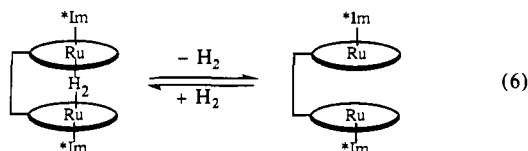
(18) Abbreviations: OEP = octaethylporphyrinato dianion; DPB = diporphyrinato-biphenylene tetraanion; THF = tetrahydrofuran; *Im = 1-*tert*-butyl-5-phenylimidazole; PPh₃ = triphenylphosphine.

Table I. Temperature Dependence of the Relaxation Rates of the Dihydrogen Ligands, Performed at 400 MHz

<i>T</i> (°C)	Ru(OEP)-(THF)(H ₂) ^a	Os(OEP)-(THF)(H ₂) ^a	Os(OEP)-(*Im)(H ₂) ^a	Ru ₂ (DPB)-(*Im) ₂ (H ₂) ^b
-75			73	
-70	44			
-60	35	130	50	441
-50	31	122		390
-45			39	
-40	28	112		288
-30	27	111	28 ^c	240
-20	26	107	dec	217
-10	25 ^c	112		
0	dec	120		159
10		124		144
20		130		134
30				133
50				180
				dec

^aIn THF-*d*₈. ^bIn toluene-*d*₈. ^cMeasured on weak signals.

this formulation have previously been published.¹⁷ Under 1 atm of H₂ approximately 5% of the diporphyrin exists as a complex with no internal ligand, suggesting that the bridging dihydrogen complex is in equilibrium with the bis 5-coordinate species, Ru₂(DPB)(*Im)₂ (eq 6). This bis 5-coordinate species can ir-



reversibly disproportionate to Ru₂(DPB)(*Im)₄ and Ru₂(DPB).¹⁹ This disproportionation causes irreversible decomposition of the dihydrogen complex over a period of weeks in solution at room temperature. Even in the presence of 1 atm of H₂, the disproportionation products do not reform the H₂ complex.

Attempts to prepare a bridged dihydrogen complex having no axial ligands or with triphenylphosphine occupying the outer coordination sites failed. Neither Ru₂(DPB) nor Ru₂(DPB)(PPh₃)₂ reacts under 1 atm of H₂. Similarly, Fe₂ and Os₂ analogues of the Ru₂(DPB)(*Im)₂(H₂) could not be prepared. Treating the Fe₂(DPB) and Os₂(DPB) with 2 equiv of the imidazole in the presence of H₂ did not result in bound dihydrogen.

Relaxation Times of the η²-Dihydrogen Ligands. Longitudinal relaxation times, *T*₁'s, have been measured for each of the dihydrogen complexes as a function of temperature²⁰ (Table I). Minimum values with respect to temperature were determined for both Ru₂(DPB)(*Im)₂(H₂) and Os(OEP)(THF)(H₂). However, both Os(OEP)(*Im)(H₂) and Ru(OEP)(THF)(H₂) decomposed before the *T*₁ vs temperature data passed through a minimum. Regardless, the near-zero slope of the *T*₁ vs temperature data for the case of Ru(OEP)(THF)(H₂) at -10 °C suggests that the *T*₁ at -10 °C is near a minimum. Plots of ln(*T*₁) vs 1/*T* for both Os(OEP)(THF)(H₂) and Ru₂(DPB)(*Im)₂(H₂) are shown in Figure 2. Both complexes display obvious minima in the *T*₁ vs temperature data and typical "V"-shaped curves consistent with a relaxation rate predominated by homonuclear dipole-dipole interactions.^{20,21} The *T*₁(min) values and the H-H distances consistent with the relaxation times (assuming H-H

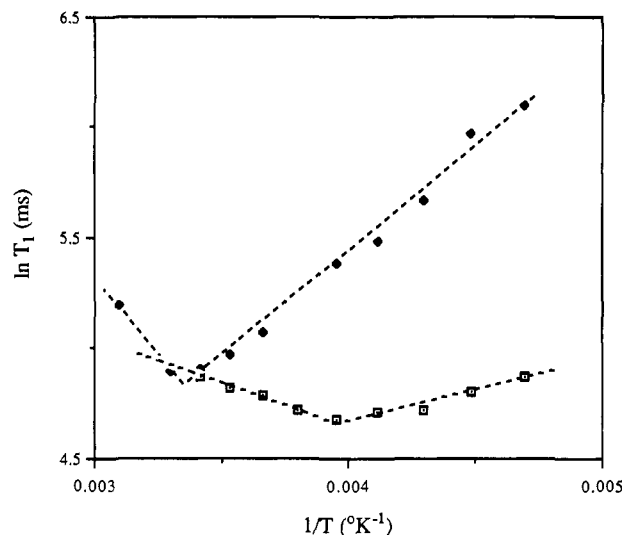


Figure 2. Plot of the ln(*T*₁) [*T*₁ measured in ms] vs reciprocal temperature [temperature measured in K] for the complexes Os(OEP)(THF)(H₂) in THF-*d*₈ (□) and Ru₂(DPB)(*Im)₂(H₂) in toluene-*d*₈ (◆) at 400 MHz. Note: Near the minimum, a simple linear relationship is not expected because the relaxation rate is not a linear function of either τ_c or τ_c^{-1} as the conditions $\omega^2\tau_c^2 \gg 1$ or $\omega^2\tau_c^2 \ll 1$ do not hold.^{20d}

Table II. *T*₁ Data Obtained at 400 MHz for the Metalloporphyrin Dihydrogen Complexes^a

complex	<i>T</i> (K)	solvent	<i>T</i> ₁ (min)	<i>r</i> ^{H-H(spin)} (Å)	<i>r</i> ^{H-H(static)} (Å)
Ru(OEP)(THF)(H ₂)	263	THF- <i>d</i> ₈	25 ms ^b	.92	1.16
Os(OEP)(THF)(H ₂)	253	THF- <i>d</i> ₈	110 ms	1.18	1.48
Os(OEP)(*Im)(H ₂)	243	THF- <i>d</i> ₈	28 ms ^c	.94	1.18
Ru ₂ (DPB)(*Im) ₂ (H ₂)	293	tol- <i>d</i> ₈	132 ms	1.21	1.53

^aThe values for *r* are calculated from the literature equations.^{22b} *r*^{H-H(spin)} assumes that the H₂ molecule is rapidly rotating, *r*^{H-H(static)} assumes that the H₂ molecule is stationary relative to the molecule. ^bAbove 263 K the hydrogen signal was too weak to measure. The *T*₁ vs. temperature data had stopped decreasing but had not begun to increase. ^cAbove 243 K the hydrogen signal was too weak to measure. *T*₁ was still decreasing with temperature.

Table III. Deuterium Coupling Constants and Isotopic Shifts Measured at 400 MHz for the Metalloporphyrin Dihydrogen Complexes^a

complex	<i>T</i> (K)	<i>J</i> _{HD}	δ(HD)	δ(H ₂)	δ(HD) - δ(H ₂)
Ru(OEP)(THF)(H ₂)	233	29.5	-31.05	-30.96	-0.09
Os(OEP)(THF)(H ₂)	293	12	-30.01	-30.00	-0.01
Os(OEP)(*Im)(H ₂)	233	27.5	-28.37	-28.24	-0.13
Ru ₂ (DPB)(*Im) ₂ (H ₂)	293	15	-38.35	-38.55	+0.20

^aChemical shifts, δ, in ppm vs. TMS; coupling constants, *J*_{HD}, in Hz.

dipolar relaxation is entirely responsible for the short relaxation times) are listed in Table II. H-H radii have been calculated assuming that the H₂ ligand either is spinning rapidly, *r*^{H-H(spin)}, or is stationary, *r*^{H-H(static)}.^{21,22b} The presence of large HD coupling constants (see Table III) is more consistent with the short H₂ distance, implying a rapidly rotating H₂ ligand.

¹H NMR Data for the η²-HD Complexes. Hydrogen deuteride complexes of the type M(OEP)(L)(HD) were synthesized analogously to the dihydrogen complexes by addition of benzoic acid-*d*₁ (85%) to the anionic hydrides. Due to exchange processes and low isotopic purity of the benzoic acid, these samples were contaminated with small quantities of the dihydrogen complex. The bridging complex Ru₂(DPB)(*Im)₂(HD) was synthesized by

(19) Collman, J. P.; Hutchison, J. E.; Guillard, R.; Lopez, M. A. Submitted for publication.

(20) Short relaxation times have been used to indicate the presence of the dihydrogen ligand. (a) Crabtree, R. H.; Hamilton, D.; Lavin, M. In *Experimental Organometallic Chemistry*; Wayda, A. L., Darensbourg, M. Y., Eds.; American Chemical Society: Washington, DC, 1987; pp 223-226. (b) Hamilton, D. G.; Crabtree, R. H. *J. Am. Chem. Soc.* **1988**, *110*, 4126-4133. (c) Luo, X.-L.; Crabtree, R. H. *Inorg. Chem.* **1990**, *29*, 2788-2791. (d) Desrosiers, P. J.; Cai, L.; Lin, Z.; Richards, R.; Halpern, J. *J. Am. Chem. Soc.* **1991**, *113*, 4173-4184. (e) V-shaped ln(*T*₁) vs 1/*T* plots also require that the rotational correlation time, τ_c , exhibit Arrhenius type behavior, i.e., $\tau_c^{-1} = Ae^{-E_a/RT}$.^{20d}

(21) Bautista, M. T.; Earl, K. A.; Maltby, P. A.; Morris, R. H.; Schweitzer, C. T.; Sella, A. *J. Am. Chem. Soc.* **1988**, *110*, 7031-7036.

(22) (a) Kubas, G. J.; Unkefer, C. J.; Swanson, B. I.; Fukushima, E. *J. Am. Chem. Soc.* **1986**, *108*, 7000-7009. (b) Earl, K. A.; Jia, G.; Maltby, P. A.; Morris, R. H. *J. Am. Chem. Soc.* **1991**, *113*, 3027-3039. (c) Bautista, M.; Earl, K. A.; Morris, R. H.; Sella, A. *J. Am. Chem. Soc.* **1987**, *109*, 3780-3782. (d) Bautista, M.; Cappellani, E. P.; Drouin, S. D.; Morris, R. H.; Schweitzer, C. T.; Sella, A.; Zubkowski, J. *J. Am. Chem. Soc.* **1991**, *113*, 4876-4887. (e) Bautista, M. T.; Earl, K. A.; Morris, R. H. *Inorg. Chem.* **1988**, *27*, 1124-1126.

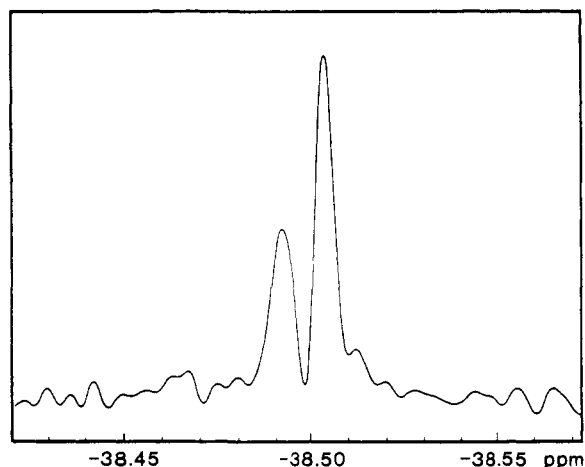


Figure 3. High-field ^1H NMR (620 MHz, C_6D_6) spectrum of the H_2 ligand signal of $\text{Ru}_2(\text{DPB})(^*\text{Im})_2(\text{H}_2)$, resolution enhanced.

saturation a benzene solution of $\text{Ru}_2(\text{DPB})$ with HD gas and then adding 2 equiv of the imidazole. The HD coupling constants and the isotopic shifts due to the deuterium substitution are given in Table III. The HD coupling constants for $\text{Os}(\text{OEP})(^*\text{Im})(\text{HD})$ and the $\text{Ru}(\text{OEP})(\text{THF})(\text{HD})$ are in the "normal" range for HD complexes, while the values for $\text{Os}(\text{OEP})(\text{THF})(\text{HD})$ and $\text{Ru}_2(\text{DPB})(^*\text{Im})_2(\text{HD})$ are more consistent with a stretched dihydrogen bond.^{10,22}

We also note the wide range of isotopic shifts caused by the deuterium substitution (-0.13 to $+0.20$ ppm). The normal direction of isotopic shift for deuterium substitution on dihydrogen complexes¹⁰ is an upfield shift upon deuterium substitution. Our monomeric dihydrogen complexes are all consistent with this observation. However, the bridged dihydrogen complex, $\text{Ru}_2(\text{DPB})(^*\text{Im})_2(\text{H}_2)$, shows a downfield or "wrong sign" shift upon deuterium substitution. To our knowledge, this is the first reported example of this "wrong sign" shift for a dihydrogen complex and is also the largest magnitude shift for deuterium substitution.

T_1 Resolved Spectroscopy. Because of the contamination of the hydrogen deuteride complexes with dihydrogen isotopomers, the HD coupling was often difficult to resolve. We have used a method to resolve these spectra, published by Earl et al.,^{22b} which takes advantage of the different relaxation times of H_2 ligands and HD ligands. Because the dipolar relaxation caused by deuterium is less efficient than the dipolar relaxation caused by protium, complexed HD signals have significantly longer relaxation times and are consequently sharper than complexed H_2 signals. As a result, we can perform a two-pulse experiment with an appropriate delay ($\tau = \ln 2 / T_1(\text{H}_2)$) to null the signal from the H_2 ligand and obtain a well-resolved, but inverted, HD ligand signal. This method was described by Kubas for the resolution of coincident hydride and dihydrogen ligand signals.^{22a}

High-Field ^1H NMR Spectra of the Bridged Dihydrogen Complex. Due to the large anisotropy of the diamagnetic susceptibility of the diporphyrin system, some alignment of the bridged dihydrogen complex occurs in strong magnetic fields.²³ This alignment results in observable dipolar H,H and H,D splittings in the high-field ^1H NMR spectra of $\text{Ru}_2(\text{DPB})(^*\text{Im})_2(\text{H}_2)$ (Figure 3) and $\text{Ru}_2(\text{DPB})(^*\text{Im})_2(\text{HD})$. The dipolar splitting, D , of the H_2 species is measured as $\pm 7.37 \pm 0.05$ Hz. The absolute sign of this splitting is unknown but can be obtained from the dipolar HD coupling. The dipolar splitting, D_{HD} , in the HD complex is superimposed on the isotropic spin-spin splitting, J_{HD} , and can only be determined by observing the total splitting of the HD complex at several field strengths. We know that J_{HD} is positive and invariant with field strength and that the dipolar splitting D_{HD} is proportional to H_0^2 (vide infra). Therefore,

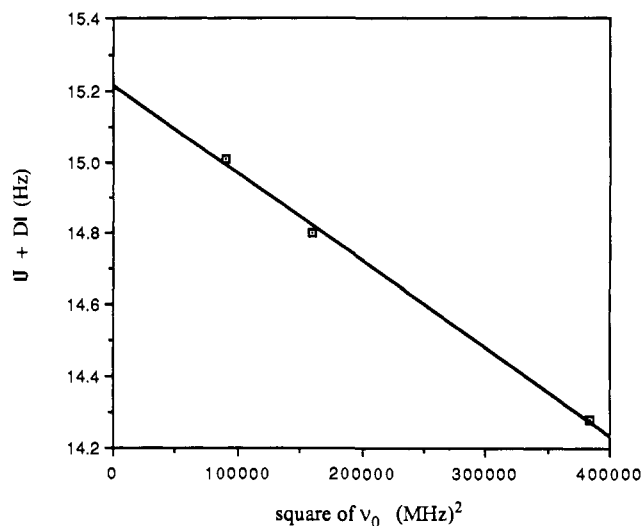
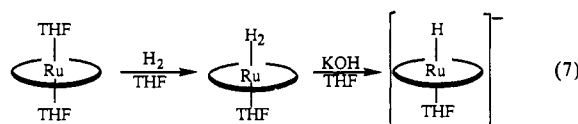


Figure 4. Total splitting $|J + D|$ of the HD signal of $\text{Ru}_2(\text{DPB})(^*\text{Im})_2(\text{H}_2)$ as a function of the square of the NMR frequency. Values were obtained on 300-, 400-, and 620-MHz spectrometers.

plotting the total splitting versus H_0^2 should yield a straight line with an intercept equal to J_{HD} . A positive slope indicates a positive D_{HD} , and a negative slope indicates a negative D_{HD} . We determined the total coupling at three different fields. The plot (Figure 4) is indeed linear and indicates a negative dipolar coupling. Implications of this observation on the determination of the structure will be discussed later.

Reactivity of the Dihydrogen Complexes. The monomeric dihydrogen complex $\text{Os}(\text{OEP})(\text{THF})(\text{H}_2)$ was effectively deprotonated with lithium diisopropylamide to yield the hydride $[\text{Os}(\text{OEP})(\text{THF})(\text{H})]^-$. Weaker bases such as proton sponge or hydroxide showed no ability to deprotonate the dihydrogen complex. We did not attempt to add strong bases to the dihydrogen complexes which were stable only at low temperature due to the extreme air and temperature sensitivity of these complexes. However, addition of KOH to a solution of $\text{Ru}(\text{OEP})(\text{THF})_2$ in THF under 1 atm of H_2 resulted in formation of $\text{K}[\text{Ru}(\text{OEP})(\text{THF})(\text{H})]$,^{15,16} presumably by deprotonation of a transient dihydrogen complex (eq 7). This suggests that KOH is a strong enough base to deprotonate the dihydrogen complex $\text{Ru}(\text{OEP})(\text{THF})(\text{H}_2)$.



All attempts to deprotonate the bridged dihydrogen complex, $\text{Ru}_2(\text{DPB})(^*\text{Im})_2(\text{H}_2)$, failed. Treatment with either proton sponge (protonated proton sponge has a $\text{p}K_a$ in water ≈ 10.7) or 2-tert-butylimino-2-diethylamino-1,3-dimethylperhydro-1,3,2-diazaphosphorine, BEMP (protonated BEMP has a $\text{p}K_a$ in water of 20.1), resulted in no reaction.²⁴ Even stirring for 10 min over excess NaH or 30 min over potassium metal in toluene gave no appreciable change. Unhindered donor bases such as butyllithium or lithium diisopropylamide readily replaced the dihydrogen ligand.

Although $\text{Ru}_2(\text{DPB})(^*\text{Im})_2(\text{H}_2)$ is stable in solution for more than a day at room temperature under 1 atm of hydrogen, the dihydrogen ligand dissociates when the solution is heated. Furthermore, dihydrogen is replaced immediately by dinitrogen to yield a bridged dinitrogen complex²⁵ and by pyridine to yield

(23) Molecular alignment in high-field NMR has recently been reviewed. Bastiaan, E. W.; MacLean, C. In *NMR Basic Principles and Progress*, Vol. 25: *NMR at Very High Field*; Diehl, P., Fluck, E., Günther, H., Kosfeld, R., Seelig, J., Eds.; Springer Verlag: New York, 1991; pp 17-43.

(24) (a) Kurasov, L. A.; Pozharskii, A. F.; Kuz'menko, V. V. *Zh. Org. Khim.* 1983, 19, 859-863. (b) Schwesinger, R.; Schlemper, H. *Angew. Chem., Int. Ed. Engl.* 1987, 26, 1167-1169. (c) The $\text{p}K_a$ values in acetonitrile for the acids of proton sponge and BEMP were taken from refs 24a and 24b, respectively, and converted to aqueous values using the equation $\text{p}K_a(\text{H}_2\text{O}) = \text{p}K_a(\text{CH}_3\text{CN}) - 7.5$ suggested by: Kristjánssdóttir, S. S.; Norton, J. R. In *Transition Metal Hydrides: Recent Advances in Theory and Experiment*; Dedieu, A., Ed.; VCH Publishers: New York, 1991; pp 309-359.

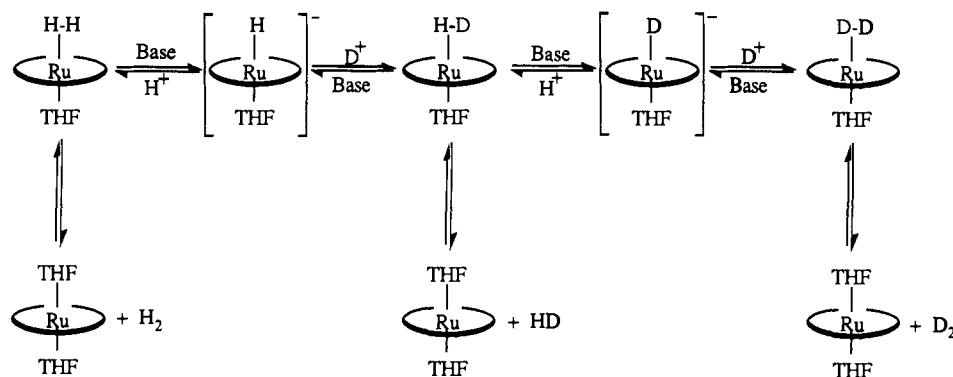


Figure 5. Proposed mechanism for Ru(OEP)(THF)₂-catalyzed H₂/D₂O exchange.

Table IV. Quantity of D₂O/H₂ Exchange as a Function of the Amount of Added KOD^a

mol of KOD/mol of Ru(OEP)(THF) ₂	H ₂ /HD/D ₂
0	1.0/0.0/0.0
12	0.10/0.30/0.60
120	0.38/0.24/0.38

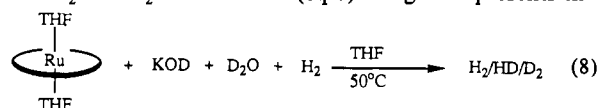
^a All solutions contained 5 μmol of Ru(OEP)(THF)₂ in 0.5 mL of THF. The KOD was added as a solution with 50 μL of D₂O. Each vial had 4 mL of Ar headspace to which 0.5 mL of H₂ (RTP) was injected. H₂/HD/D₂ ratios were measured by GC after stirring for 160 min at 50 °C.

Ru₂(DPB)(pyridine)₂(*Im)₂ which has the two pyridine ligands bound in the cavity of the diporphyrin.¹⁹ The rate of displacement of hydrogen is sensitive to the nature of the incoming ligand; after 5 min of purging with Ar gas, more than 25% of the dihydrogen complex remains, whereas replacement with dinitrogen occurs immediately. Replacement by deuterium gas occurs without scrambling to give Ru₂(DPB)(*Im)₂(D₂); formation of Ru₂(DPB)(*Im)₂(HD) was not observed.

Cyclic voltammetry of the Ru₂(DPB)(*Im)₂(H₂) in *o*-difluorobenzene²⁶ was unsuccessful due to the rapid dissociation of the H₂ ligand when not rigorously kept under 1 atm of dihydrogen. We have not been able to reduce the dihydrogen complex with either potassium metal or potassium naphthalide. This behavior is similar to that of the bridged dinitrogen complex Ru₂(DPB)(*Im)₂(N₂).²⁵ One-electron oxidation of the dihydrogen complex with [FeCp₂]PF₆ yields a complex with a paramagnetic ¹H NMR spectrum. To determine whether oxidation of this complex by one electron would create an acidic dihydrogen ligand, Ru₂(DPB)(*Im)₂(H₂) was oxidized using [FeCp₂]PF₆ in the presence of the hindered base 2,6-lutidine. No protonated 2,6-lutidine was observed. We suspect that one-electron oxidation labilizes the H₂.²⁷

H₂/D₂O Exchange. We previously reported¹⁵ that in the presence of Ru(OEP)(THF)₂ and KOH in THF isotopic exchange

between H₂ and D₂O is observed (eq 8). Figure 5 presents the



mechanism we proposed for this H/D exchange. This mechanism has now been further substantiated by our recent discovery of the intermediate Ru(OEP)(THF)(H₂), in addition to the finding that this complex can easily be deprotonated by KOH. As suggested by the mechanism, this exchange exhibits a maximum with respect to the amount of added KOH.¹⁵ This pH dependence is depicted in Table IV. The maximum extent of exchange occurs for the intermediate value of added base. Hydrogenase enzymes are also known to catalyze such H/D exchange and exhibit a similar pH profile.⁶

Electrochemistry in H₂-Saturated Solutions of Metalloporphyrins Adsorbed on Graphite. Ru(OEP)(THF)₂ was adsorbed onto an edge plane graphite electrode, EPGE, and this electrode was placed in a 0.1 M aqueous solution of NaOH. Substantially larger oxidation waves were noted when the aqueous solution was saturated with H₂ rather than Ar. In the absence of the ruthenium catalyst, the EPGE displayed no oxidation current under H₂. Further studies demonstrated that [Ru(OEP)]₂ shows behavior identical to Ru(OEP)(THF)₂, but the [Ru(OEP)]₂ catalytic oxidation waves are much more intense.²⁸ All of the following experiments were performed with [Ru(OEP)]₂ on the EPGE.

The electrochemistry of [Ru(OEP)]₂ on the EPGE was performed under both Ar and H₂ (Figure 6). Under Ar, a surface wave is observed centered at -0.67 V vs NHE (Figure 6a). Cyclic voltammograms under H₂ display large anodic currents on both

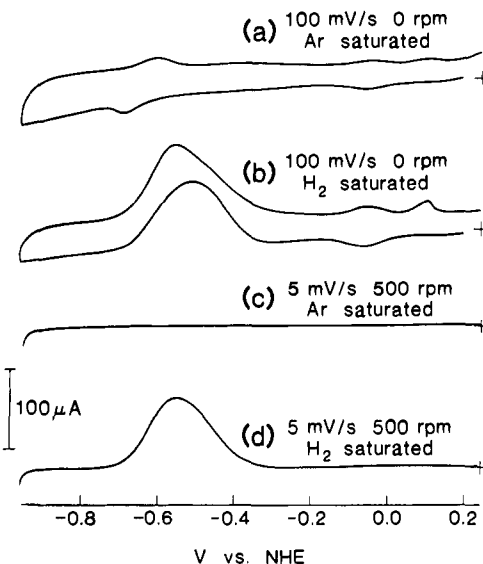


Figure 6. Electrochemistry of [Ru(OEP)]₂ adsorbed onto a graphite disk and immersed in aqueous 0.1 M NaOH.

(25) (a) Collman, J. P.; Hutchison, J. E.; Lopez, M. A.; Guillard, R.; Reed, R. A. *J. Am. Chem. Soc.* **1991**, *113*, 2794-2796. (b) Collman, J. P.; Hutchison, J. E.; Lopez, M. A.; Guillard, R.; Reed, R. A. Manuscript submitted for publication.

(26) O'Toole, T. R.; Younathan, J. N.; Sullivan, B. P.; Meyer, T. J. *Inorg. Chem.* **1989**, *28*, 3923-3926.

(27) One-electron oxidation of the metal in transition metal dihydrogen complexes has been suggested to increase the acidity of the dihydrogen ligand but also to significantly increase the lability of the bound dihydrogen.^{22d}

(28) (a) We believe that the active form of the catalyst is the deposited dimer for both the Ru(OEP)(THF)₂ and [Ru(OEP)]₂ treated electrodes. The activity of the deposited Ru(OEP)(THF)₂ increases drastically after being cycled to 0.6 V vs SCE and more closely matches that of the deposited [Ru(OEP)]₂. One possible explanation is a dimerization of the Ru(OEP)(THF)₂ upon oxidation. Such a dimerization of the resulting ruthenium(III) fragments might be thermodynamically favored because a very strong Ru-Ru triple bond might be formed to yield [Ru(OEP)]₂²⁺. This species has been isolated in solution.⁴⁷ (b) A similar dimerization on a graphite electrode has been observed for rhodium phthalocyanines. Tse, Y.-H.; Seymour, P.; Kobayashi, N.; Lam, H.; Leznoff, C. C.; Lever, A. B. P. *Inorg. Chem.* **1991**, *30*, 4453-4459.

Table V. T_1 , J_{HD} , Calculated r_{HH} , and Decomposition Data for Four OEP Metalloporphyrin Dihydrogen Complexes^a

ligand	metal	
	ruthenium	osmium
*Im	Ru(OEP)(*Im)(H ₂) not obsd at -78 °C	Os(OEP)(*Im)(H ₂) $T_1(\text{min}) = 28$ ms $J_{HD} = 27.5$ Hz $r_{HH(\text{spin})} = 0.94$ Å dec at -20 °C
THF	Ru(OEP)(THF)(H ₂) $T_1(\text{min}) = 25$ ms $J_{HD} = 29.5$ Hz $r_{HH(\text{spin})} = 0.92$ Å dec at -30 °C	Os(OEP)(THF)(H ₂) $T_1(\text{min}) = 108$ ms $J_{HD} = 12$ Hz $r_{HH(\text{spin})} = 1.18$ Å dec at >20 °C

^a These data are compiled from Tables I–III.

the anodic sweep and the cathodic sweep (Figure 6b). These oxidation currents are much larger than the surface wave observed under Ar. The intensity of the wave in Figure 6b relative to the surface wave implies that this wave is due to a diffusional process and not a surface species. This is additionally demonstrated by the slow scan rotating disk voltammograms in Figure 6, parts c and d; in the absence of H₂ no oxidation current is seen at a 5 mV/s scan rate, whereas a hydrogen saturated solution under the same conditions shows a well-defined oxidation current.

We find only a slight rotation rate dependence on the peak current. The peak current is insensitive to changes in rotation rates above 500 rpm, demonstrating that the oxidation is not diffusion limited and indicating a slow step on the electrode surface. Additionally, the observation of an anodic wave during both the anodic scan and the cathodic scan of the cyclic voltammogram indicates incomplete consumption of the electroactive species at the electrode surface, again implying that the electrochemical process responsible for this wave is slow.

Curiously, we note the absence of a steady state current in the slow scan rotating disk experiment under hydrogen. The decrease in the oxidation current after the plateau indicates that the dihydrogen oxidation process is being inactivated at more positive potentials. This is strictly an inactivation of the catalyst and not a destruction of the catalyst because subsequent scans through the wave show identical behavior.

The oxidation current is also pH dependent. When identical experiments were performed in solutions in the pH range 10–13, the oxidation wave was found to move to a more positive potential and the current to decrease in intensity with decreasing pH, until the oxidation is nearly unobservable at pH = 10. We also observe a decrease in the intensity of the oxidation current while changing pH from 13 to 14. Addition of 1 M KBr to solutions at pH 13 also suppressed the oxidation current. Addition of 1 drop of pyridine (<0.1% (v/v)) to the pH 13 solution completely suppressed the oxidation current.

The bridging dihydrogen complex, Ru₂(DBP)(*Im)₂(H₂), and the dimeric precursor Ru₂(DPB) were adsorbed onto an EPG electrode and cyclic voltammograms run under both Ar and H₂ in 0.1 M NaOH. No additional oxidation current was observed under H₂ for either species.

Discussion

Factors Affecting Dihydrogen Character in Monomeric Dihydrogen Complexes. We have prepared several monomeric dihydrogen complexes of metalloporphyrins to determine the effect that the metal and trans ligand have on the dihydrogen character of the ligand. We chose these ligand and metal systems also to illustrate the effect of two metals on the dihydrogen ligand in the bridging dihydrogen complex, Ru₂(DPB)(*Im)₂(H₂). Three metalloporphyrin dihydrogen complexes were prepared; the characteristics are summarized in Table V. As several other authors have discussed,^{22c,d,29} we have found that osmium binds dihydrogen more tightly than ruthenium, resulting in the osmium

dihydrogen complexes which are more stable and more hydridic than their ruthenium analogues. This is indicated by the higher $T_1(\text{min})$ values, lower J_{HD} values, and greater stability of the osmium complexes relative to their ruthenium analogues. The trends in stability¹⁰ and especially $T_1(\text{min})$ ²⁰ are well documented to qualitatively indicate a lengthening of the HH bond in the dihydrogen complexes. Small J_{HD} values have also been used²² to qualitatively indicate shorter H–D bonds. However, some authors have found data which contrast with this intuitive relationship.^{11g,21} The data presented in Table V present additional evidence in favor of a smooth correlation between J_{HD} and r_{HH} for a family of closely related complexes; the complexes having the largest J_{HD} values also have the smallest T_1 values and, consequently, the shortest calculated H–H bonds.

Curiously, we have also discovered that the better σ -donor ligand, *Im, destabilizes the dihydrogen complexes relative to the poorer σ -donor ligand, THF. This is implied by the increased stability of the complexes with THF trans to the dihydrogen ligand, as well as their larger $T_1(\text{min})$ and smaller J_{HD} relative to the complexes with *Im trans to the dihydrogen ligand. Because greater electron density at the metal usually increases the strength of the metal–dihydrogen interaction,^{10,20b} the labilizing effect of the imidazole may be due to its greater π -acidity relative to THF.

The trends that we observe indicate that Ru(OEP)(*Im)(H₂) should be the least stable and most dihydrogen-like complex of the series. Indeed, we see that even at -78 °C this complex cannot be observed. The observation that protonation of the K[Ru(OEP)(*Im)(H)] results in loss of H₂ and formation of the asymmetric Ru(OEP)(*Im) complex implies that protonation forms a very unstable dihydrogen complex which decomposes even at -78 °C. The implication of these trends on the geometry of the bridged complex Ru₂(DPB)(*Im)₂(H₂) will be discussed below.

Contributions to T_1 Other than H–H Dipolar Broadening. The T_1 values display the expected dependence on temperature, assuming homonuclear dipole–dipole relaxation predominates²⁰ (Table I; Figure 2). However, this does not necessarily imply that the only contribution to the relaxation is a dipole–dipole interaction between the bound protons. Effects from chemical shift anisotropy and from interactions with ligand protons may also be significant. Thus the observed $T_1(\text{min})$, $T_{1,\text{obs}}$, will be composed of contributions from relaxation due to chemical shift anisotropy, $T_{1,\text{csa}}$, and relaxation due to interaction with other ligand protons, $T_{1,\text{L}}$, as well as the dipolar relaxation due to the bound protons, $T_{1,\text{H–H}}$ (eq 9).^{20d}

$$\frac{1}{T_{1,\text{obs}}} = \frac{1}{T_{1,\text{H–H}}} + \frac{1}{T_{1,\text{csa}}} + \frac{1}{T_{1,\text{L}}} \quad (9)$$

Because of the rigid structure that the porphyrin imposes in the molecule, no ligand protons are closer than 4 Å to the dihydrogen ligand. Calculations using the method of Desrosiers^{20d} suggest that the contribution to relaxation from ligand protons should be <5%. Effects from chemical shift anisotropy, however, may be significant for porphyrins because as the porphyrin tumbles in solution the H₂ ligand feels a large fluctuating magnetic field due to the aromatic ring current. However, due to the relatively low field strength at which the T_1 values were measured and the interference between the magnetic dipole and chemical shift anisotropy relaxation mechanisms, this effect should not influence the T_1 values (vide infra). Therefore, $T_{1,\text{obs}}$ should very closely approximate $T_{1,\text{H–H}}$. The consequence of this is that the equations relating T_1 to the H–H bond distance should be valid for these complexes and the radii listed in Table II should very closely approximate the interproton distance of the hydrogen ligand.

In addition, the dipolar relaxation time for the H₂ ligand of Ru₂(DPB)(*Im)₂(H₂) will be unaffected by the anisotropic tumbling which causes the dipolar splitting, even though the T_1 equation assumes isotropic tumbling. This is due to the small magnitude of molecular alignment responsible for the observed splitting. For Ru₂(DPB)(*Im)₂(H₂) in solution, a dipolar splitting of -7.37 Hz is measured whereas solid-state NMR spectroscopy of dihydrogen complexes, where no tumbling occurs, gives dipolar splittings on the order of hundreds of kHz.³⁰ Thus, the overall

(29) Amendola, P.; Antoniutti, S.; Albertin, G.; Bordignon, E. *Inorg. Chem.* 1990, 29, 318–324.

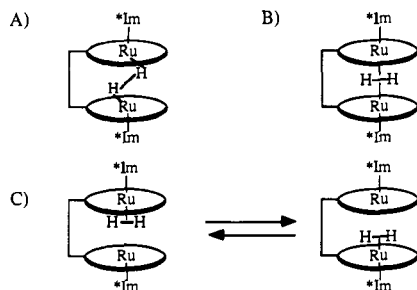


Figure 7. Possible binding modes for the complex $\text{Ru}_2(\text{DPB})(^*\text{Im})_2(\text{H}_2)$: (A) the hydrogen ligand bisects the Ru–Ru axis at an acute angle; (B) the hydrogen ligand is at or near parallel to the porphyrin planes; (C) the hydrogen ligand is undergoing rapid site exchange between the two ruthenium centers.

degree of alignment necessary to cause the small splitting we observe is less than one in 10 000 and the tumbling is virtually isotropic. The actual degree of alignment, S_z , will be calculated below.

Orientation of H_2 in Bridged Dihydrogen Complex. The spectroscopic data presented¹⁷ for $\text{Ru}_2(\text{DPB})(^*\text{Im})_2(\text{H}_2)$ demonstrate that only one molecule of dihydrogen is bound between the two metal centers. Though bimetallic complexes containing dihydrogen ligands are known,³¹ to our knowledge this is the first complex that binds dihydrogen between the two metals. As discussed in our previous communication,¹⁷ the spectroscopic data are consistent with three possible modes of binding (Figure 7). The fact that the two porphyrins remained equivalent on the NMR time scale, even at -80°C , suggested that structures A and B are the most likely candidates.¹⁷ Further evidence favoring structures A and B is found in the trends demonstrated by the monomeric dihydrogen complexes.

The instability of the putative monomeric $\text{Ru}(\text{OEP})(^*\text{Im})(\text{H}_2)$ suggests that both ruthenium centers of the dimeric complex must be acting in concert on the dihydrogen ligand. A single ruthenium porphyrin with a trans imidazole is not capable of forming a stable η^2 -dihydrogen complex at room temperature. In order to obtain enough interaction between the complex and the dihydrogen ligand, both binding sites, acting simultaneously, must be present. This argument suggests that the structure shown in Figure 7C should be unstable. An even more compelling argument *against* the structure in Figure 7C follows from the trends noted in Table V. These trends suggest that an H_2 ligand under the influence of only one ruthenium porphyrin with a trans imidazole ligand [i.e., $\text{Ru}(\text{OEP})(^*\text{Im})(\text{H}_2)$] would have unusually high J_{HD} values and very low $T_1(\text{min})$ values. Because the $\text{Ru}_2(\text{DPB})(^*\text{Im})_2(\text{H}_2)$ shows the exact opposite trends, we conclude that both ruthenium centers are acting in concert on the dihydrogen ligand.

The flexibility of the M_2DPB systems (M–M distances from 3.8 Å for $\text{Cu}_2(\text{DPB})$, with both Cu atoms bound in the porphyrin plane,³² to 4.85 Å for $\text{Ru}_2(\text{DPB})(^*\text{Im})_2(\text{N}_2)$ ²⁵ have been measured) permits this concerted binding of various sized substrates. Presumably, the metals could pull toward each other, out of the porphyrin planes, to permit binding of small substrates. Unfortunately, this flexibility does not allow us to preclude either structure A or B in Figure 7 through a consideration of the bond distances involved. Consequently, we sought a method to determine the angle between the porphyrin planes and the H–H axis.

Zilm³⁰ has recently used solid-state ^1H NMR spectroscopy as a tool for structural determinations of dihydrogen complexes, but the quantities required for these experiments exceed the amounts that we are able to synthesize conveniently. Because high-field

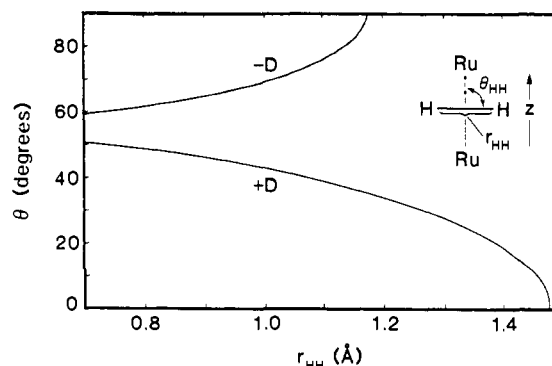


Figure 8. Plot of the possible values of Θ_{HH} versus r_{HH} .

^1H NMR spectroscopy has been shown to be valuable in determining structural information for systems with large anisotropies in their diamagnetic susceptibility tensors,²³ we recorded the high-field ^1H NMR spectrum of the bridged dihydrogen complex. The splitting observed in Figure 3 results from an alignment of the porphyrin plane with the magnetic field, resulting in a dihydrogen ligand which no longer tumbles anisotropically. The degree of alignment, S_z , is given by eq 10.³³

$$S_z = \langle \frac{1}{2} \cos^2 \Theta_z - \frac{1}{2} \rangle = \Delta\chi H^2 / 15kT \quad (10)$$

Here, Θ_z is the angle between the magnetic field direction and the axis of maximum diamagnetic susceptibility of the molecule (parallel to the Ru–Ru axis), and $\Delta\chi$ is the anisotropy of the susceptibility. $\Delta\chi$ for the molecule may be estimated closely by summing the known magnetic susceptibility anisotropies of the porphyrin rings³⁴ ($-10.5 \times 10^{-28} \text{ cm}^3$), phenyl³⁵ ($-1.0 \times 10^{-28} \text{ cm}^3$), imidazole rings ($-0.7 \times 10^{-28} \text{ cm}^3$), and biphenylene bridging group³⁶ ($-1.4 \times 10^{-28} \text{ cm}^3$) using the summation

$$\Delta\chi_{\text{M}} = \sum \Delta\chi_i (\frac{1}{2} \cos^2 \Theta_g - \frac{1}{2}) \quad (11)$$

where Θ_g is the angle between the molecular z axis and the normal to the rings of the constituent groups. Thus, the value $-19.1 \times 10^{-28} \text{ cm}^3$ is obtained. At 296 K and a magnetic field of 145 600 G (620 MHz), this gives $S_z = -6.61 \times 10^{-5}$. The dipolar interaction, D_{HH} , is given by³³

$$D_{\text{HH}} = -\frac{\gamma_{\text{H}}^2 h}{2\pi^2 r_{\text{HH}}^3} (\frac{1}{2} \cos^2 \Theta_{\text{HH}} - \frac{1}{2}) \quad (12)$$

where γ_{H} is the proton gyromagnetic ratio, r_{HH} is the interproton distance, and Θ_{HH} is the angle between the molecular z axis and the HH internuclear axis. Substituting for the known constants yields the relation

$$-\frac{(3 \cos^2 \Theta_{\text{HH}} - 1/2)}{r_{\text{HH}}^3} = (6.30 \times 10^{22}) D_{\text{HH}} \quad (13)$$

The splitting observed for the H_2 signal at 620 MHz is $\pm 7.37 \pm 0.05 \text{ Hz}$ (Figure 3), which is $3D_{\text{HH}}/2$, so that the relation

$$\frac{-(3/2 \cos^2 \Theta_{\text{HH}} - 1/2)}{r_{\text{HH}}^3} = \pm 0.309 \times 10^{24} \quad (14)$$

is obtained. The curves in Figure 8 trace the possible combinations of Θ_{HH} and r_{HH} . In this figure, the upper lobe corresponds to negative values of D_{HH} and the lower to positive values.

The sign of D could be determined from the high-field spectra of the HD complex. In this case, the hydrogen is expected³⁷ to yield a signal which is a 1:1:1 triplet, with spacing $J_{\text{HD}} + D_{\text{HD}}$. Since D_{HD} varies as the square of the magnetic field, the plot of

(30) Zilm, K. W.; Merrill, R. A.; Kummer, M. W.; Kubas, G. J. *J. Am. Chem. Soc.* **1986**, *108*, 7837–7839.

(31) (a) Hampton, C.; Dekleva, T. W.; James, B. R.; Cullen, W. R. *Inorg. Chim. Acta* **1988**, *145*, 165–166. (b) Arliguie, T.; Chaudret, B.; Morris, R. H.; Sella, A. *Inorg. Chem.* **1988**, *27*, 598–599. (c) Hampton, C.; Cullen, W. R.; James, B. R. *J. Am. Chem. Soc.* **1988**, *110*, 6918–6919.

(32) Fillers, J. P.; Ravichandran, K. G.; Abdalmuhdi, I.; Tulinsky, A.; Chang, C. K. *J. Am. Chem. Soc.* **1986**, *108*, 417–424.

(33) Bastiaan, E. W.; VanZijl, P. C. M.; MacLean, C.; Bothner-By, A. A. *Annu. Rep. NMR Spectrosc.* **1987**, *19*, 35–37.

(34) Bothner-By, A. A.; Gayathri, C.; VanZijl, P. C. M.; MacLean, C.; Lai, J. J.; Smith, K. M. *Magn. Reson. Chem.* **1985**, *23*, 935–938.

(35) Bothner-By, A. A.; Gayathri, C.; VanZijl, P. C. M.; MacLean, C. *J. Magn. Reson.* **1984**, *56*, 456–462.

(36) Landolt-Bornstein *NSII/16* **1988**, 403–444.

(37) Emaley, J. W.; Lindon, J. C. In *NMR Spectroscopy Using Liquid Crystal Solvents*; Pergamon Press: New York, 1975.

measured splittings against H_0^2 (Figure 4) is linear. The intercept gives J_{HD} . The D_{HD} at 620 MHz should be given by D_{HH} times γ_D/γ_H or $\sim \pm 0.75$ Hz, in agreement with Figure 4. Finally, since the splitting at high fields is smaller than that at low fields, the signs of J_{HD} and D_{HD} must be opposite. J_{HD} is positive, therefore D_{HD} (and D_{HH}) are negative, and the upper lobe of Figure 8 applies.

Given r_{HH} as determined from $T_1(\text{min})$ and the relationship between Θ_{HH} and r_{HH} displayed in Figure 8, it is clear that Θ_{HH} must be very close to 90° , i.e., the H_2 axis is very nearly parallel to the porphyrin planes. Thus, Figure 7B corresponds most nearly to the induced geometry.

The pattern of differing line widths in the H_2 and HD complexes deserves comment. In the case of the H_2 doublet, the high-frequency line is broader. The source of such differential broadening has been elucidated by Mackor and MacLean;³⁸ it arises from interference between the magnetic dipole and chemical shift anisotropy relaxation mechanisms. The ratio of the line widths indicates that the relative contributions of dipolar and shift anisotropy interactions are about 6:1, and the ratio of the line widths or apparent intensities are thus $(6 + 1)^2:(6 - 1)^2$ or about two to one. The longitudinal relaxation is also affected, and the decay will be slightly biexponential. However, the measurements of $T_1(\text{min})$ upon which the HH distance is based will not be particularly affected because (1) the average relaxation of both lines is measured and (2) the measurements were performed at lower field where the chemical shift anisotropy contribution is strongly reduced. Analysis indicates that the broadening of the high-frequency line in the doublet will occur regardless of whether the HH axis is parallel or perpendicular to the molecular z axis. The triplet proton signal from the HD complex shows a different pattern. The central line is the narrowest, the high-frequency line is slightly broader, and the low-frequency line is the broadest. The pattern is rationalized as follows: (1) Electric quadrupole relaxation of the deuterium is most effective from the +1 and -1 levels, causing the outer lines of the proton triplet to be broader than the central line.³⁹ (2) Interference between chemical shift anisotropy and magnetic dipolar interaction broadens the low-frequency line of the triplet relative to the high-frequency line provided J_{HD} and D_{HD} are opposite in sign and $|J_{HD}| > |D_{HD}|$. Thus, the pattern confirms nicely the opposite sign as deduced above.

Deuterium Isotope Effect on Chemical Shift of Dihydrogen Complexes. We noted a large range of deuterium isotope effects ($\delta_{HD} - \delta_{HH}$) on the shifts of the dihydrogen complexes upon deuterium substitution. This included the "wrong-sign" value for $Ru_2(\text{DPB})(^*Im)_2(H_2)$. Three reasonable explanations for the wrong-sign shift were suggested. (1) Cleavage of the H_2 ligand to a dihydride changes the sign of the shift. (2) Bridging dihydrogen ligands will intrinsically have a "wrong-sign" shift. (3) Hydrogen-deuteride binds to a metal center asymmetrically, placing the proton and deuterium in different regions of the porphyrin ring current. The first explanation seems unlikely given several reports of normal upfield shifts of the proton of a metal dihydride upon substitution of one of the hydrides with deuteride.⁴⁰ This is the same behavior that is observed for deuterium substitution on methyl protons.⁴¹ However, it cannot be excluded because a similar "wrong-sign" shift has been observed upon deuterium substitution on the polyhydride $OsH_4(\text{PTol}_3)_3$.^{20d} The second explanation is unlikely because the bridging dihydrogen complex has no other anomalous characteristics, nor does this explanation have any theoretical basis. We favor the third explanation, an asymmetrically bound HD molecule with the Ru-D

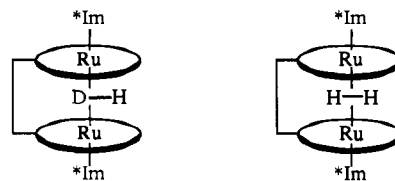


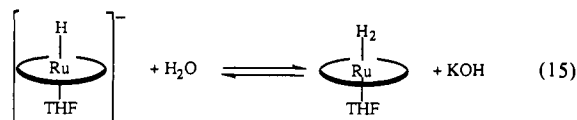
Figure 9. $Ru_2(\text{DPB})(^*Im)_2(\text{HD})$ with an asymmetrically bound HD. The HD molecule rotates about a point closer to the deuterium than the hydrogen. The proton on the HD complex is shifted further from the center of the porphyrin than the protons on the H_2 complex.

bond distances shorter than the Ru-H bonds (Figure 9). This is quite reasonable because deuterium is known to form shorter bonds than does hydrogen due to its lower zero-point energy. Additionally, HD will prefer to rotate about its center of gravity (which is closer to the deuterium than the proton) rather than the geometric center. Both of these effects will favor a structure that places the proton on HD farther from the center of the porphyrin ring than the protons on H_2 , which is symmetrically bound. If the proton on HD is shifted farther from the center of the metalloporphyrin, it will experience less of the induced magnetic field from the ring current of the porphyrin, imparting a downfield shift to the proton on HD relative to H_2 . All HD complexes should contain asymmetric bound HD. However, only for metalloporphyrins would this asymmetry be expected to cause a large enough chemical shift to overcome the normal upfield shift resulting from the deuterium.

Table III shows that the two dihydrogen complexes with short H-H distances, $Ru(\text{OEP})(\text{THF})(H_2)$ and $Os(\text{OEP})(^*Im)(H_2)$, display normal upfield shifts upon deuteration but that the two complexes with stretched H-H ligands, $Os(\text{OEP})(\text{THF})(H_2)$ and $Ru_2(\text{DPB})(^*Im)_2(H_2)$, show little shift or a "wrong-sign" shift, respectively. Because a stretched H-D ligand implies stronger metal-hydride interactions, we would expect the asymmetry to be more amplified for these cases. For $Os(\text{OEP})(\text{THF})(H_2)$, the ring current effect does not quite overcome the normal isotopic shift, but for $Ru_2(\text{DPB})(^*Im)_2(H_2)$, the effect of two porphyrins easily surmounts the normal isotopic shift to yield an overall downfield shift upon deuterium substitution. This theory could be easily tested by observing the deuterium resonance of the HD complex which should experience an upfield shift. Such studies were hampered by the inherent sensitivity problems associated with deuterium NMR spectroscopy, compounded by the relatively low concentrations we necessarily employ due to the costly nature and solubility limitations of the DPB complexes.

Acidity of Dihydrogen Complexes. Several groups have reported dihydrogen complexes with relatively high acidities.¹¹ Deprotonation of dihydrogen complexes which can be synthesized by addition of hydrogen to a metal with a labile ligand or an open coordination site represents a key step in the heterolytic activation of dihydrogen. Consequently, we examined the acidity of the dihydrogen complexes $Os(\text{OEP})(\text{THF})(H_2)$, $Ru(\text{OEP})(\text{THF})(H_2)$, and $Ru_2(\text{DPB})(^*Im)_2(H_2)$. We were not able to deprotonate the bridging dihydrogen complex with bases having pK_a values of up to 20.1. Additionally, the $Os(\text{OEP})(\text{THF})(H_2)$ was difficult to deprotonate, i.e., lithium diisopropylamide was required. These low acidities are consistent with the enhanced hydridic character of these dihydrogen complexes.

The dihydrogen complex $Ru(\text{OEP})(\text{THF})(H_2)$ is inferred as the intermediate in the reaction that forms $K[Ru(\text{OEP})(\text{THF})(H)]$ from $Ru(\text{OEP})(\text{THF})_2$, hydrogen, and KOH (eq 7). This implies that KOH is a strong enough base to deprotonate $Ru(\text{OEP})(\text{THF})(H_2)$. We have also shown¹⁶ that H_2O in large concentrations is a strong enough acid to protonate $K[Ru(\text{OEP})(\text{THF})(H)]$ (eq 15). This indicates that the pK_a values of $Ru(\text{OEP})(\text{THF})(H_2)$ and H_2O are very similar.



(38) Mackor, E. L.; MacLean, C. *Prog. NMR Spectrosc.* **1967**, *3*, 129-157.

(39) (a) Pople, J. A. *Mol. Phys.* **1958**, *1*, 168-174. (b) Suzuki, M.; Kubo, M. *Mol. Phys.* **1964**, *7*, 201-209.

(40) (a) Heinekey, D. M.; Millar, J. M.; Koetzle, T. F.; Payne, N. G.; Zilm, K. W. *J. Am. Chem. Soc.* **1990**, *112*, 909-919. (b) Baird, G. J.; Davies, S. G.; Moon, S. D.; Simpson, S. J.; Jones, R. H. *J. Chem. Soc., Dalton Trans.* **1985**, 1479-1486.

(41) Hanson, P. E. *Annu. Rep. NMR Spectrosc.* **1983**, *15*, 105-225.

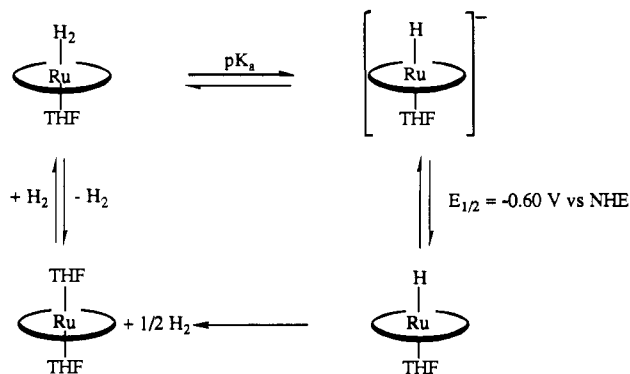


Figure 10. Thermodynamic cycle for the oxidation of dihydrogen utilizing Ru(OEP)(THF)₂ as a catalyst. All steps are verified. Only the pK_a of the dihydrogen complex is unknown.

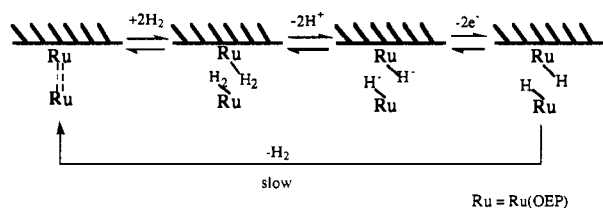


Figure 11. Scheme I for the oxidation of dihydrogen at a graphite surface treated with [Ru(OEP)]₂.

H₂ Oxidation Catalysis. Because each step shown in Figure 10 has been demonstrated in solution,¹⁶ Ru(OEP)(THF)₂ should be capable of catalyzing hydrogen oxidation. We have deposited Ru(OEP)(THF)₂ on a graphite electrode and measured a diffusional anodic current under H₂ in basic conditions, which we attribute to the catalytic oxidation of dihydrogen. We have also found that the dimeric species [Ru(OEP)]₂ is most likely the active catalyst. The catalysis is completely inhibited by traces of pyridine; apparently the required coordination site is blocked or the surface ruthenium dimer structure may be disrupted.⁴² Additionally, catalysis turns off at higher pH; perhaps hydroxide ion, in high concentration, is another inhibitory ligand. This hypothesis is supported by the fact that 1 M KBr also suppressed the oxidation current.

As one possibility for the catalytic mechanism, we suggest the scheme depicted in Figure 11. Figure 11 shows a mechanism on the surface analogous to the solution studies we have performed on Ru(OEP)(THF)₂, as depicted in Figure 10. First, it involves the coordination of two molecules of dihydrogen to form two dihydrogen complexes in a cofacial orientation. Though this step has not been observed in solution for the dimer, the adsorption of the dimer onto the surface may change the properties of the [Ru(OEP)]₂ to allow a hydrogen addition analogous to the addition of dihydrogen to Ru(OEP)(THF)₂. The next step incorporates deprotonation of these acidic dihydrogen ligands. The acidity of this dihydrogen ligand will enforce a lower limit on the pH at which the catalysis may occur. This is consistent with our finding that the oxidation current decreases substantially over the pH range from 11 to 10. This mechanism requires the deprotonation *before* the oxidation for two reasons: (1) Prior oxidation of the metal center would presumably render the already labile dihydrogen ligand extremely labile.²⁷ (2) Only by deprotonating the dihydrogen ligand does the oxidation potential of the complex become positive enough to permit the catalysis at the potentials we have noted (the oxidation potential of the Ru(OEP)(THF)(H)⁻ in THF solution is ca. -0.60 V vs NHE,⁴⁴ whereas neutral Ru^{II}

(42) Quinhydrone on the surface of graphite has been noted to act as a reversible hydrogen electrode.⁴³ The absence of an oxidation current in the absence of [Ru(OEP)]₂ and the inhibition of the catalyst by very low concentrations of pyridine make this a very unlikely possibility for the catalysis that we observe. Pyridine would not be expected to act as an inhibitor for quinhydrone catalyzed hydrogen oxidation.

(43) Puri, B. R. *Chem. Phys. Carbon* 1970, 6, 191–282.

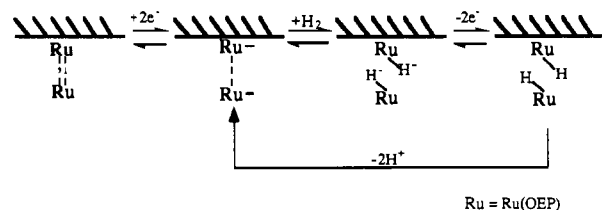


Figure 12. Scheme II for the oxidation of dihydrogen at a graphite surface treated with [Ru(OEP)]₂.

porphyrin complexes are oxidized at ca. 0 V vs NHE⁴⁵). Finally, we propose binuclear reductive elimination of dihydrogen from the two metal centers. We have documented this step in our solution studies.¹⁶ Note that this step results in an unusual stoichiometry.



This stoichiometry has not been verified for our electrode studies; there is no apparent way to do so.

This mechanism is at first attractive because all of the steps have analogies in solution and the slow electrode kinetics can be explained by a binuclear step which has been found¹⁶ to be slow in solution. Additionally, the potential of the electrode process occurs near the reversible potential for K[Ru(OEP)(THF)(H)]^{0/-}, which is proposed to be an intermediate in this mechanism. However, it does not explain why the hydrogen oxidation shuts down at potentials only slightly more positive than the potential corresponding to the current maximum. If we invoke the mechanism in Figure 11, then at potentials where neutral Ru^{II} complexes are oxidized to Ru^{III} (ca. 0 V vs NHE⁴⁵) we would expect the affinity for dihydrogen to decrease and consequently see the dihydrogen oxidation current fall off. Instead, we see the oxidation current fall off 0.5 V more negative than expected. Perhaps the interaction of the surface with [Ru(OEP)]₂ moves the Ru^{II/III} potential more negative than expected. Given our reservations with this mechanism, we consider another possible mechanism as shown in Figure 12.

In this second mechanism the first step is proposed to be the reduction of the [Ru(OEP)]₂ by two electrons to form the ruthenium “dimer dianion”. We believe that the surface wave noted under Ar at -0.67 V vs NHE may be the reduction of the neutral dimer to the “dimer dianion”.⁴⁶ Next, this dimer dianion oxidatively adds hydrogen across its single bond to form two ruthenium(II) hydrides. This step has been shown to occur in THF solution.¹⁶ Subsequently, these anionic hydrides are proposed to be oxidized and then deprotonated, returning the catalyst to the “dimer dianion” form. This mechanism is also consistent with the existence of a lower limit to the pH at which this process will occur, that being the pK_a of the ruthenium(III) hydride. This mechanism also explains why the oxidation shuts down at a potential only slightly more positive than the current plateau. At potentials near or more negative than the first surface reduction wave there should be substantial quantities of the dimer dianion, but at potentials more positive than this, the catalyst would exist as the neutral [Ru(OEP)]₂ which we have shown does not oxidatively add dihydrogen.

Given the problems associated with each mechanism, we are not ready to state which if either of these mechanisms is most

(44) This value was estimated by using the redox potential for K[Ru(OEP)(THF)(H)] vs FeCp₂⁺⁰ in THF as reported in ref 16 and correcting for FeCp₂⁺⁰ vs NHE. Bard, A. J.; Faulkner, L. R. In *Electrochemical Methods: Fundamentals and Applications*; John Wiley and Sons, Inc.: New York, 1980.

(45) Kadish, K. M. In *Progress in Inorganic Chemistry*; Lippard, S. H., Ed.; John Wiley and Sons, Inc.: New York, 1986; Vol. 34, pp 435–605.

(46) Identifying the oxidation state change of this surface wave is difficult given that the adsorbed species may be modified on the surface. By comparison to solution studies,⁴⁷ which show the first reduction of the dimer to occur at ca. -0.8 V vs NHE, we believe it may correspond to the reduction of the dimer.

(47) Collman, J. P.; Prodoliet, J. W.; Leidner, C. R. *J. Am. Chem. Soc.* 1986, 108, 2916–2921.

likely. The problems of ligation with oxygenated groups⁴³ on the edge plane graphite and the problems associated with the obvious interaction of the graphite with the catalyst further complicate these analyses. Determining the form of the catalyst on the surface of graphite is thus very difficult. Consequently we are beginning to synthesize porphyrins with substituents which can be covalently attached to noble metal or transparent glass electrodes. This should eliminate many of the ambiguities associated with the graphite surface.

The reason for presenting the above two mechanisms at this time is for the purpose of comparing and contrasting possible mechanisms for transition metal complex catalyzed hydrogen oxidation. First, note that both mechanisms require the activation of dihydrogen, but through very different means: in scheme I hydrogen is activated to heterolytic cleavage by making the dihydrogen ligand more acidic; in scheme II hydrogen is activated by overall homolytic cleavage. Second, both mechanisms require a bimolecular stage: in scheme I because of a binuclear reductive elimination of dihydrogen; in scheme II because of a homolytic cleavage (oxidative addition) of dihydrogen by two metal centers. Third, both mechanisms require the removal of both protons and electrons, but in different orders: in scheme I protons are removed before electrons; in scheme II electrons are removed before protons. Fourth, both mechanisms will have a lower limiting pH: in scheme I the limiting pH is set by the pK_a of a dihydrogen complex; in scheme II the limiting pH is set by the pK_a of the metal hydride. Solutions having a pH lower than these pK_a values would not allow the oxidation of dihydrogen. Finally, both mechanisms should work only in a limited potential range because oxidizing the active form of the catalyst will decrease the catalyst's affinity for dihydrogen.

A seldom noted fact concerning the overpotentials in electrocatalysis needs to be considered here. The thermodynamic potential for hydrogen oxidation is governed by eq 17, the Nernst equation for proton reduction:

$$E_{1/2}(\text{vs NHE}) = 0.000 \text{ V} - 0.059 (\text{pH}) \text{ V} \quad (17)$$

At pH = 13, the thermodynamic potential for H₂ oxidation is -0.77 V, whereas we find the half-wave potential for the catalyzed hydrogen oxidation occurs at -0.62 V. Thus, our system operates with a 0.15-V overpotential. Because there is an overpotential for hydrogen oxidation using this catalytic system, it is *thermodynamically impossible to reduce protons using the microscopic reverse of the above hydrogen oxidation mechanism*. Performing such a process would mean operating at a 0.15-V "underpotential". Consequently, to find a catalyst for proton reduction, the operating potential of the catalyst must be changed by altering the central metal or ancillary ligands.

The more hydridic bridged complex Ru₂(DPB)(*Im)₂(H₂) displays no catalytic activity for hydrogen oxidation. At pH = 13, no significant deprotonation of the bridging dihydrogen ligand occurs; our solution studies with various bases suggest its pK_a to be >20. The acidity of the dihydrogen ligand could in principle be increased by oxidation; however, such oxidation appears to destroy the affinity of the bimetallic site for dihydrogen. Such a dilemma illustrates the delicate balance of these mechanisms.

Conclusions

We have shown that metalloporphyrins of various electronic and steric constitution are capable of binding dihydrogen. The use of the porphyrin ligand has greatly simplified the synthesis and characterization of these dihydrogen complexes because of the lack of readily accessible cis-coordination sites, the absence of ligand protons near enough to affect the dipolar relaxation of the dihydrogen ligand, and the ease with which we were able to modify the trans ligand. Ru(OEP)(THF)(H₂) is especially interesting because deprotonation of this complex readily occurs to form an active hydride which is capable of reducing pyridinium salts and one-electron oxidants.¹⁶ These factors, coupled with its capacity for catalyzing the H₂-D₂O exchange reaction, suggest that this complex is a reasonable model for the non-porphyrinic hydrogenase reactivity. The intermediacy of the [Ru(OEP)-

(THF)(H)]⁻ in all these reactions is consistent with the suggestion by Krasna and Rittenberg that the active site of the hydrogenase enzymes contains a hydride formed from heterolytic activation of dihydrogen.

We have also demonstrated catalysis of dihydrogen oxidation and presented models which may be useful in designing dihydrogen oxidation catalysts. It is apparent that, in designing hydrogen oxidation catalysts, the order of proton and electron removal, as well as the limiting values for the potentials and pH, as governed by the thermodynamic potentials, will need to be considered.

Experimental Section

General Considerations. Commercially available solvents and reagents were purchased and used as received unless otherwise noted. Solvents and reagents for use in the inert atmosphere box were further purified before use. Toluene, benzene, and THF were distilled from sodium benzophenone ketyl under argon. After introduction into the inert atmosphere box, these solvents were purged for 15 min with the box atmosphere to remove any residual oxygen. Tetrahydrofuran for routine use was monthly repurified in small amounts by vacuum transfer from its sodium benzophenone ketyl solution. All other liquid reagents were degassed in Schlenk-ware by 3 freeze-pump-thaw cycles before introduction into the box. Deuterated solvents were scrupulously dried prior to use in the inert atmosphere box. Benzene-*d*₆, toluene-*d*₈, and tetrahydrofuran-*d*₈ were purified by forming the Na/K benzophenone ketyl in a Schlenk flask and vacuum transferring to another Schlenk flask for storage. THF-*d*₈ was redried every 2 weeks. Tetrabutylammonium hexafluorophosphate was twice recrystallized from ethanol, dried in a vacuum oven (10⁻² Torr, 100 °C), and stored in the inert atmosphere drybox. Orthodifluorobenzene was transferred from CaH₂ prior to use. Ferrocene was purified by sublimation before use and [FeCp₂]PF₆ was synthesized according to literature procedures.⁴⁸

The metalloporphyrin hydrides;¹⁶ the metalloporphyrin dimers Ru₂(DPB),⁴⁹ Os₂(DPB),⁵⁰ Fe₂(DPB),⁵¹ and Ru₂(DPB)(PPh₃)₂;⁴⁹ 1-*tert*-butyl-5-phenylimidazole, *Im;⁵² and Ru(OEP)(THF)₂;^{16,53} were prepared according to the literature procedures. Hydrogen (99.999%) and deuterium (99.9%) were used as received from Liquid Carbonic. Hydrogen-deuteride gas was used as prepared by dropping D₂O onto a slurry of sodium hydride in benzene and passing the gas through a pipet packed with activated alumina. The HD flow was controlled by controlling the D₂O addition rate. The isotopic purity was >80% as determined by gas chromatography.

All manipulations of the metalloporphyrin hydrides and dihydrogen complexes were performed in a Vacuum/Atmospheres Co. inert atmosphere dry box equipped with an HE493 Dri-Train and operated under an argon atmosphere. Oxygen levels (≤5 ppm) were monitored by a Vacuum/Atmospheres Co. AO316-C trace oxygen analyzer. Solvent manipulations and degassing of air-sensitive samples were performed on a bench top vacuum line in Schlenk flasks and NMR tubes fitted with J. Young Teflon valves and O-ring vacuum adapter fittings. ¹H NMR data were recorded on Varian XL-400 and GEM-200 instruments. High-field ¹H NMR experiments were recorded on the 620-MHz instrument at Carnegie Mellon University. All electrochemical experiments employed a Princeton Applied Research 175 wave generator, and the 173 Potentiostat/Galvanostat. All electrochemical experiments in nonaqueous solution were performed in the inert atmosphere box. The working electrode (platinum disk, *r* ≈ 0.5 mm) was circumscribed by the platinum wire loop auxiliary electrode in a 2-mL compartment separated from the reference electrode by a luggin capillary. The reference electrode was a Ag wire that was referenced to ferrocene at the conclusion of the experiment. Water for aqueous electrochemical experiments was purified to 18 MΩ cm using a Barnstead Nanopure II water filter.

Electrochemical Studies on Graphite. Electrochemical studies of metalloporphyrins adsorbed onto edgeplane graphite electrodes were performed outside the drybox in a 9-cm-diameter flat-bottom cell fitted with three joints, one each for the graphite working electrode, gold auxiliary electrode, and saturated calomel reference electrode. A syringe needle was inserted through a Teflon stopcock to purge with argon and hydrogen gas. The cell was filled to a depth of 3 cm with the backing electrolyte

(48) Yang, E. S.; Chan, M.-S.; Wahl, A. C. *J. Phys. Chem.* **1975**, *79*, 2049-2052.

(49) Collman, J. P.; Kim, K.; Leidner, C. R. *Inorg. Chem.* **1987**, *26*, 1152-1157.

(50) Collman, J. P.; Garner, J. M. *J. Am. Chem. Soc.* **1990**, *112*, 166-173.

(51) Collman, J. P.; Wagenknecht, P. S. Unpublished.

(52) vanLeusen, A. M.; Schaart, F. J.; vanLeusen, D. *Rec. J. R. Neth. Chem. Soc.* **1979**, *98*, 258-262.

(53) Venburg, G. D. Ph.D. Dissertation, Stanford University, 1990.

solution of the appropriate pH and purged for 30 min with argon. A 7.5-mm-diameter edgeplane graphite electrode was admitted into the drybox and immersed in a 10^{-5} to 10^{-4} M solution of $[\text{Ru}(\text{OEP})_2]$ in benzene for 2–3 min to adsorb the porphyrin onto the surface.⁵⁴ The electrode was removed from the solution and allowed to dry in the drybox atmosphere. The electrode was removed from the drybox in a Schlenk flask under Ar, removed from the flask and quickly attached to a Pine instruments ASR2 rotator and admitted to the argon purged solution. Cyclic voltammetry and a slow scan (5 mV/s) rotating disk experiment were performed under the Ar atmosphere. The solution was subsequently purged for 15 min with hydrogen and the experiments repeated. The experiments were then repeated under Ar then H_2 using the same electrode. Identical experiments were performed by adsorbing benzene solutions of $\text{Ru}_2(\text{DPB})$ and $\text{Ru}_2(\text{DPB})(^*\text{Im})_2(\text{H}_2)$ onto the graphite surface. The potentials were corrected for the potential of SCE vs NHE.

In Situ Preparation of the Dihydrogen Complexes. (a) $\text{Os}(\text{OEP})(\text{THF})(\text{H}_2)$. $\text{K}[\text{Os}(\text{OEP})(\text{THF})(\text{H})]$, 5 μmol in 1 mL of $\text{THF}-d_8$, was treated with excess benzoic acid, ~ 2 equiv. The dihydrogen complex was formed in 30% yield with the contaminants identified as $[\text{Os}(\text{OEP})_2]$ and $\text{Os}(\text{OEP})(\text{THF})_2$. The dihydrogen complex was characterized by ^1H NMR spectroscopy, including T_1 values for the dihydrogen ligand and J_{HD} values for the HD isotopomer (see text). ^1H NMR ($\text{THF}-d_8$, 20 °C, ppm): porphyrinic resonances, H_{meso} 9.29 (s, 4 H), CH_2 3.83 (m, 16 H), CH_3 1.81 (t, 24 H); $\text{Os}(\text{H}_2)$ -30.00 (br s).

(b) $\text{Ru}(\text{OEP})(\text{THF})(\text{H}_2)$. An NMR tube attached to a rotationally balanced J. Young Teflon valve was obtained from R. J. Brunfeldt Co. Slightly below the point at which the valve seats, 13 μL of a toluene solution containing benzoic acid (50 mg of $\text{PhCOOH}/1000 \mu\text{L}$) was deposited and dried under reduced pressure, being careful to keep the 5 μmol of PhCOOH residue near the top of the tube. A $\text{THF}-d_8$ solution of $\text{K}[\text{Ru}(\text{OEP})(\text{THF})(\text{H})]$, 5 μmol , was carefully transferred to the bottom of the tube without disturbing the PhCOOH residue. The valve was seated and the sealed tube brought out of the inert atmosphere box and immediately submerged in a dry ice/acetone bath. After being cooled, the sample was shaken to ensure complete mixing of the hydride with the benzoic acid, at which time the sample changed colors from orange to red. The cooled sample was inserted into the NMR probe which had already been cooled and shimmed on a $\text{THF}-d_8$ sample at -70 °C. The dihydrogen complex was contaminated with $\sim 15\%$ $\text{Ru}(\text{OEP})(\text{THF})_2$. The dihydrogen complex was characterized by ^1H NMR spectroscopy, including T_1 values for the dihydrogen ligand and J_{HD} values for the HD isotopomer (see text). ^1H NMR ($\text{THF}-d_8$, -60 °C, ppm): porphyrinic resonances, H_{meso} 9.73 (s, 4 H), CH_2 4.04 (m, 8 H), 3.91 (m, 8 H), CH_3 1.87 (t, 24 H); $\text{Ru}(\text{H}_2)$ -30.91 (br s).

(c) $\text{Os}(\text{OEP})(^*\text{Im})(\text{H}_2)$. $\text{K}[\text{Os}(\text{OEP})(^*\text{Im})(\text{H})]$ was protonated at low temperature, analogous to the synthesis for $\text{Ru}(\text{OEP})(\text{THF})(\text{H}_2)$. The dihydrogen complex was contaminated with $\sim 15\%$ $\text{Os}(\text{OEP})(^*\text{Im})(\text{THF})$. The dihydrogen complex was characterized by ^1H NMR

spectroscopy, including T_1 values for the dihydrogen ligand and J_{HD} values for the HD isotopomer (see text). ^1H NMR ($\text{THF}-d_8$, -60 °C, ppm): porphyrinic resonances, H_{meso} 9.01 (s, 4 H), CH_2 3.78 (m, 16 H), CH_3 1.76 (t, obscured); $\text{Os}(\text{H}_2)$ -28.26 (br s); imidazole resonances, *p*-phenyl 6.98 (t, 1 H); *m*-phenyl 6.82 (t, 2 H); *o*-phenyl 5.98 (d, 2 H); $\text{H}_{\text{imidazole}}$ 1.36 (s, 1 H), 0.92 (s, 1 H); *tert*-butyl 0.15 (s, 9 H).

(d) $\text{Ru}_2(\text{DPB})(^*\text{Im})_2(\text{H}_2)$. Under an argon atmosphere, a solution of Ru_2DPB , 0.7 μmol , in benzene- d_6 or toluene- d_8 (0.5 mL of a 1.4 mM stock solution) was bubbled for 5 min with hydrogen. Two equivalents of 1-*tert*-butyl-5-phenylimidazole ($^*\text{Im}$; 58 μL of a 26.5 mM stock solution in benzene- d_6) was added and hydrogen bubbling was continued for 2 min. ^1H NMR (C_6D_6 , ppm): porphyrinic resonances, H_{meso} 8.81 (s, 2 H), 8.72 (s, 4 H); biphenylene 7.15 (2 H, obscured by residual solvent peak), 7.06 (d, 2 H), 6.85 (t, 2 H); $-\text{CH}_2\text{CH}_3$ 4.38 (m, 8 H), 3.91 (m, 8 H); $-\text{CH}_3$ 3.50 (s, 12 H), 3.25 (s, 12 H); $-\text{CH}_2\text{CCH}_3$ 1.81 (t, 12 H), 1.61 (t, 12 H). Imidazole resonances, *p*-phenyl 6.21 (t, 2 H); *m*-phenyl 5.99 (t, 4 H); *o*-phenyl 4.38 (d, 4 H); $\text{H}_{\text{imidazole}}$ -0.34 (s, 2 H), -0.40 (s, 2 H); *tert*-butyl -0.86 (s, 18 H); $\text{Ru}-\text{H}_2$ -38.6 (bs, 2 H).

Attempted Synthesis of $\text{Ru}(\text{OEP})(^*\text{Im})(\text{H}_2)$. $\text{K}[\text{Ru}(\text{OEP})(^*\text{Im})(\text{H})]$ was protonated in $\text{THF}-d_8$ at -78 °C analogously to the preparation of $\text{Ru}(\text{OEP})(\text{THF})(\text{H}_2)$. Only $\text{Ru}(\text{OEP})(\text{THF})(^*\text{Im})$ was observed as the product. The low-temperature protonation was also performed in toluene- d_8 . Only $\text{Ru}(\text{OEP})(^*\text{Im})$ was observed as the product.

Longitudinal Relaxation Times, T_1 . Relaxation times were measured on a Varian XL-400 using the inversion recovery method. The XL-400 software computes a T_1 by assuming peak height is related to peak intensity by a single constant for all delay times and fitting peak height versus delay time to the equation describing T_1 . We also calculated T_1 values for two cases by printing the dihydrogen resonances for a series of delay times and integrating by cutting and weighing the peaks. When these values were fitted to the T_1 equation, good agreement ($\pm 12\%$) with the computer-calculated T_1 values was obtained.

$\text{H}_2/\text{D}_2\text{O}$ Exchange. In the inert atmosphere box under argon, five 1-dram vials were charged with 0.5 mL of THF , 5 μmol of $\text{Ru}(\text{OEP})(\text{THF})_2$, and a stir bar and sealed with a Teflon cap fitted with a valve through which a syringe needle could be inserted to sample the headspace. Two solutions containing 60 μmol KOD in 50 μL of D_2O (2800 μmol) and two containing 600 μmol KOD in 50 μL of D_2O were prepared and added to the vials. To the remaining vial, 50 μL of D_2O was added. Each vial was injected with 0.5 mL of H_2 gas. The vials were taken from the inert atmosphere box and stirred vigorously at 50 °C for 160 min. Headspace samples from each vial were analyzed for H_2 , HD, and D_2 gas using gas chromatography.¹⁶ Isotope ratios for each of the identical runs were averaged.

Acknowledgment. We thank Dr. Robert Hembre for helpful discussions. We thank the National Science Foundation, National Institutes of Health, and the Gas Research Institute for financial support. The 620-MHz NMR spectra were obtained at the NMR Facility for Biomedical Studies, supported by the National Institutes of Health Grant RR00292. This is contribution No. 8521 from the Division of Chemistry and Chemical Engineering, California Institute of Technology.

(54) (a) Collman, J. P.; Hendricks, N. H.; Leidner, C. R.; Ngameni, E.; L'Her, M. *Inorg. Chem.* **1988**, *27*, 387–393. (b) Collman, J. P.; Denisevich, P.; Konai, Y.; Marrocco, M.; Koval, C.; Anson, F. C. *J. Am. Chem. Soc.* **1980**, *102*, 6027–6036.